Advances in Geo-Energy Research

Original article

In-situ hydrogen production from natural gas reservoirs and gas separation by graphite packing: Process simulation and experimental study

Bennet Nii Tackie-Otoo¹, Mohamed Mahmoud^{1®}*, Arshad Raza^{1®}*, Shirish Patil¹, Mobeen Murtaza², Muhammad Shahzad Kamal², Umer Zahid^{3,4}

Keywords:

In-situ hydrogen production natural gas carbon storage graphite membrane process simulation

Cited as:

Tackie-Otoo, B. N., Mahmoud, M., Raza, A., Patil, S., Murtaza, M., Kamal, M. S., Zahid, U. *In-situ* hydrogen production from natural gas reservoirs and gas separation by graphite packing: Process simulation and experimental study. Advances in Geo-Energy Research, 2025, 18(2): 165-179. https://doi.org/10.46690/ager.2025.11.06

Abstract:

The generation of hydrogen in-situ from hydrocarbon reservoirs has emerged as a carbon neutral technology for fossil fuel-based hydrogen production. This technology has been extensively investigated for heavy oil reservoirs through in-situ combustion gasification. This study proposes in-situ hydrogen generation from depleted gas reservoirs and assess graphite gravel packing for selective hydrogen production with underground carbon storage. The viability of this hydrogen generation process was accessed through process simulation, followed by experimental investigation and molecular simulation of the selective production of hydrogen through graphite. Equilibrium and kinetic models reproduced measured effluent fractions, confirming their reliability. The simulation outcomes reveal that higher temperature and steam-to-carbon ratio increase hydrogen yield/purity, whereas high pressure favors methanation. This necessitates elevated temperatures beyond the usual reaction temperature under reservoir conditions. Longer residence time and judicious catalyst loading improve conversion while limiting diminishing returns. Adiabatic simulation yields lower hydrogen purity than isothermal but better reflects field behavior. Reservoir mineralogy governs outcomes as quartz-rich rocks inhibit hydrogen production by steam reforming, while clays/feldspars reported elsewhere can be catalytic. The experimental results showed that graphite can be used as gravel pack in the production well to produce hydrogen and retain carbon dioxide underground. Literature report indicates that high compaction can further enhance separation significantly reducing the carbon emission associated with hydrogen production from fossil fuels.

1. Introduction

The rising global energy demand, fueled by population growth, industrialization, and urbanization, highlights the urgent need for sustainable energy solutions to mitigate climate

change and air pollution (Satpute and Suryabhan, 2024). Fossil fuels have long dominated global energy supply but are responsible for severe environmental degradation and biodiversity loss. Renewable sources like solar, wind, and geoth-

Yandy Scientific Press *Corresponding author.

E-mail address: bennetnii.tackieotoo@kfupm.edu.sa (B. N. Tackie-Otoo); mmahmoud@ kfupm.edu.sa (M. Mahmoud); arshad.raza@kfupm.edu.sa (A. Raza); patil@kfupm.edu.sa (S. Patil); mobeen@kfupm.edu.sa (M. Murtaza). 2207-9963 © The Author(s) 2025.

Received July 26, 2025; revised September 10, 2025; accepted October 1, 2025; available online October 6, 2025.

¹Department of Petroleum Engineering, King Fahd University of Petroleum & Minerals (KFUPM), Dhahran 31261, Saudi Arabia

²Center for Integrative Petroleum Research (CIPR), King Fahd University of Petroleum & Minerals (KFUPM), Dhahran 31261, Saudi Arabia

³Department of Chemical Engineering, King Fahd University of Petroleum and Minerals, Dhahran 31261, Saudi Arabia

⁴Interdisciplinary Research Center for Membranes & Water Security, King Fahd University of Petroleum & Minerals (KFUPM), Dhahran 31261, Saudi Arabia

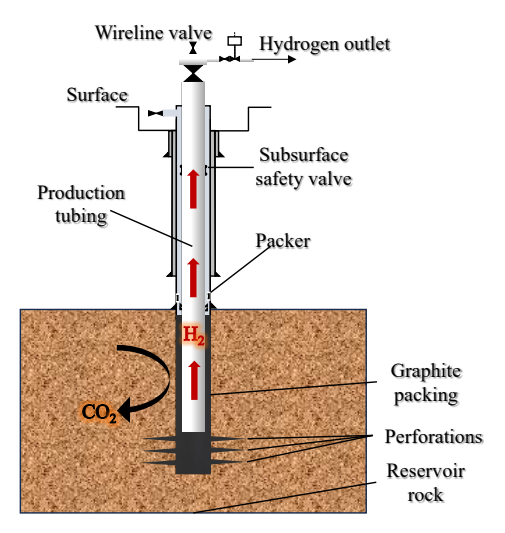


Fig. 1. Schematic representation of graphite gravel packing.

ermal offer cleaner alternatives (Gupta et al., 2018; Bashiru et al., 2024), yet challenges such as high capital costs, energy intermittency, and policy limitations hinder widespread adoption (Lv, 2023). Hydrogen (H₂) stands out as a clean and flexible energy carrier with diverse applications (Tarkowski and Uliasz-Misiak, 2022). Growing environmental concerns and fossil fuel depletion have intensified interest in hydrogen energy (Aravindan and Kumar, 2023). Therefore, advancing efficient and sustainable H₂ production technologies is vital to meet global decarbonization goals and ensure a secure, low-carbon energy future.

Hydrogen can be produced through several methods, with fossil fuel-based processes currently dominating global production. Steam methane reforming (SMR) alone contributes about 50% of total H₂ supply (Soltani et al., 2021). Other established methods include partial oxidation, autothermal reforming, and coal gasification (Kumar et al., 2021). Although these routes are mature and cost-effective, they emit large quantities of CO₂, making them inconsistent with climate goals (Liguori et al., 2020; Aravindan and Kumar, 2023). Blue hydrogen, produced by integrating carbon capture and storage into hydrocarbon reforming, offers a transitional low-carbon option (AlHumaidan et al., 2023; Massarweh et al., 2023). However, inefficiencies such as incomplete CO₂ capture, high operating costs, and long-term storage risks (Howarth and Jacobson, 2021; Riemer and Duscha, 2023) limit its effectiveness. Consequently, these constraints have driven research toward alternative, truly low-carbon hydrogen production pathways that ensure both environmental and economic sustainability.

In-situ hydrogen production (IHP), the generation of H₂ directly within hydrocarbon reservoirs, has emerged as a promising route for clean and efficient hydrogen generation (Yang et al., 2022; Ifticene et al., 2024). This method produces hydrogen within subsurface formations, avoiding many surface processing challenges (Ikpeka et al., 2020). IHP naturally confines CO₂ and other byproducts within geological formations, minimizing emissions (Aftab et al., 2022). Moreover, leveraging existing reservoir infrastructure and subsurface thermal conditions enhances efficiency and reduces capital

costs, making it an attractive sustainable option (Ifticene et al., 2023). One notable technique is *in-situ* combustion gasification (ISCG), which injects air/oxygen and steam into heavy oil reservoirs to oxidize part of the crude oil, generating heat for hydrogen-forming reactions such as thermolysis, aqua thermolysis, coke gasification, and the water-gas shift (WGS) (Hajdo et al., 1985; Ifticene and Yuan, 2024). Hydrogen is extracted via downhole membranes, while CO₂ remains sequestered (Ifticene et al., 2023).

Field-scale operations such as *in-situ* combustion (ISC) and toe-to-heel air injection have confirmed the feasibility of generating hydrogen through (ISCG) (Ifticene et al., 2023). Several studies have since explored deploying conventional ISC methods, originally developed for heavy oil recovery, for hydrogen generation via gasification (as summarized in Table A1). The first dedicated ISCG pilot was launched by Proton Technologies in 2017 (Ifticene et al., 2023). Natural gas reservoirs are now being evaluated as promising candidates for similar IHP applications due to their higher hydrogento-carbon ratios, greater global energy reserves, and existing adaptable infrastructure (Tong et al., 2018; Algayyim et al., 2024; Alekhina et al., 2025). Furthermore, steam reforming and partial oxidation of natural gas are mature technologies (Nikolaidis and Poullikkas, 2017). However, comprehensive experimental and field-scale studies remain necessary to validate reaction mechanisms, reservoir suitability, economic viability, and operational safety.

Gillick and Babaei (2024) proposed a downhole completion tool capable of converting natural gas wells into hydrogen production systems by gasifying natural gas within the wellbore rather than the reservoir. Afanasev et al. (2024) and Mukhina et al. (2024) also studied the feasibility of IHP in natural gas reservoirs. They reported that using water-soluble catalysts and optimizing the steam-to-carbon (S/C) ratio could significantly enhance H2 yield. Contrary to the reform approaches, Yan et al. (2024) demonstrated that methane cracking via electromagnetic heating can achieve up to 91 mol% H₂ due to the catalytic behavior of rock minerals. However, most studies used pure methane feeds, ignoring real natural gas compositions that contain heavier hydrocarbons, which can lower the H₂/CO ratio and cause carbon deposition (Dybkjaer and Christensen, 2001). Tackie-Otoo et al. (2025) extended this research to multi-component natural gas, showing that equilibrium (stoichiometric) models overpredict yields due to neglecting side reactions, while experiments revealed lower yields limited by methanation and low S/C ratios.

The present study advances this work using both equilibrium (non-stoichiometric) and kinetic models. These models are used to evaluate the thermodynamic limits and reaction kinetics of the IHP process. The effects of natural gas composition and reservoir mineralogy on hydrogen generation efficiency are also examined. The models are validated with experimental data to ensure accuracy. Finally, the results are used to identify realistic process constraints and propose strategies for optimizing IHP. This study also evaluates the use of graphite packing as a downhole filter to selectively produce hydrogen while retaining CO₂ in the reservoir (Fig. 1). The graphite packing exploits the stronger CO₂ adsorption

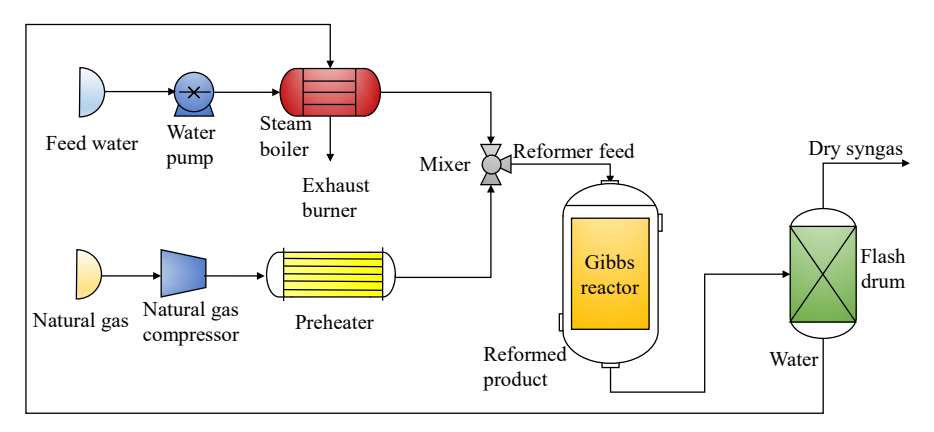


Fig. 2. Process simulation flow diagram for in situ natural gas steam reforming using Gibbs reactor.

and slower diffusion compared to H₂, which diffuses more rapidly and aids separation as reported in several studies (summarized in Table A2). Graphite-based membranes demonstrate promising H₂/CO₂ selectivity under ideal, single-gas conditions, yet real-mixture separations are much lower, underlining the challenge of translating ideal performance to practical environments (Schulz et al., 2014). Based on insights from these studies, this study deploys experimental setup with cores made to mimic the proposed scenarios is used to investigate the selective production of hydrogen from underground reservoirs. This approach eliminates the need for expensive membrane separation and carbon capture technologies by utilizing the reservoir itself for *in situ* separation and storage. Furthermore, the retained CO₂ could aid in maintaining reservoir pressure, thereby facilitating efficient H₂ withdrawal.

2. Methodology

In this study, methane steam reforming (SR) was simulated under reservoir-relevant conditions, using experimental data from Mukhina et al. (2024) for model validation. The experimental setup employed pure methane as a feedstock to simplify the analysis; however, this does not fully represent the gas composition typically encountered in depleted natural gas reservoirs. Therefore, the validated models were further extended to assess the effect of natural gas composition on H₂ production. In addition, a series of parametric studies and sensitivity analysis were conducted to explore the optimal operating conditions for *in-situ* hydrogen generation, aiming to improve process efficiency and adaptability for subsurface applications. The final part involved experimental procedure to test the selective permeation of H₂ and CO₂ mixture through a graphite gravel pack. The permeation and self-diffusivity of H₂ and CO₂ through a graphite core were both investigated.

2.1 Process simulation of hydrocarbon reform

A comprehensive steady-state simulation of the natural gas SR process was conducted using the process simulation code "ASPEN Plus 9". In the study by Mukhina et al. (2024), steam reforming of methane was experimentally investigated under simulated reservoir conditions using both real reservoir core samples and inert α -Al₂O₃ as porous medium. In this

simulation study, the focus was placed on the inert α -Al₂O₃ experiments, as the influence of rock minerals on hydrogen generation requires detailed characterization before being accurately incorporated into simulation models. Currently, there is no consensus in the literature regarding the specific effects of reservoir rock minerals on the hydrogen production process. Experiments were conducted at temperatures of 500, 600 and 800 °C with S/C ratios of 1 and 4, under a pressure of 8 MPa. The experimental setup involved a tubular reactor having an internal volume of 32.5 cm³ filled with porous medium (average porosity $\sim 48.40\%$). The methane was injected into the porous model at 1.4 L/h flow rate. Aiming to replicate the effluent composition reported by Mukhina et al. (2024), two distinct reactor models were implemented: (i) a nonstoichiometric equilibrium model using the RGibbs reactor and (ii) a kinetic model using the RPlug reactor, configured with Langmuir-Hinshelwood-Hougen-Watson reaction kinetics. The former is a zero-dimensional model while the latter includes reactor dimensions as well as catalyst properties.

2.1.1 Non-stoichiometric model description

The non-stoichiometric model employs a Gibbs free energy minimization approach as detailed in Supplementary B. The RGibbs reactor block in ASPEN Plus computes the equilibrium composition without requiring reaction stoichiometry. The Peng Robinson equation of state was selected in the property method section for accurate thermodynamic predictions of light gases. Initially, the process flowsheet was defined (Fig. 2), specifying the feedstock and key unit operations. Detailed process parameters, including temperature, pressure, flow rates, and compositions for each stream were based on data from Mukhina et al. (2024). The steam flow rate is specified using a calculator block based on the required S/C ratio. Subsequent investigations were conducted at a 700 °C and S/C ratio of 3.5. The effects of other natural gas components and impurities are investigated using natural gas compositions of different natural gas reservoirs as presented in Table B1. The effect of rock minerals is also investigated using composition reported Afanasev et al. (2024) and Mukhina et al. (2024). The rock sample is composed of quartz (60.65%), feldspar (12.83%), clay minerals (15.54%), calcite (5.41%), dolomite (1.1%), halite (4.27%) and pyrite (0.20%).

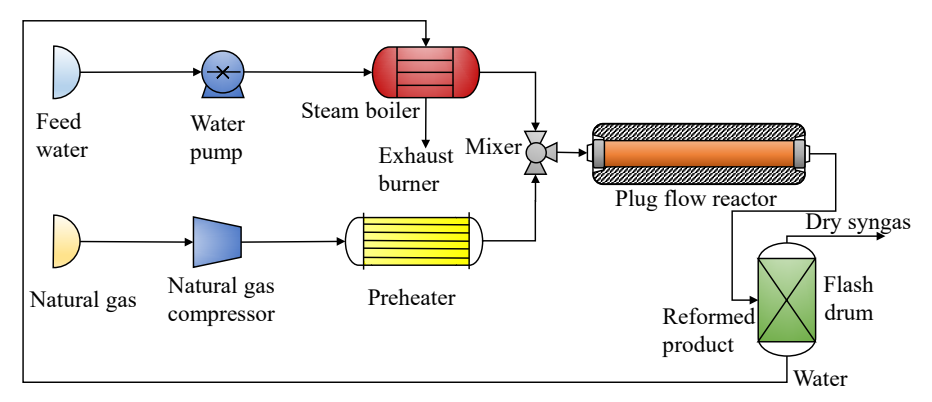


Fig. 3. Process simulation flow diagram for in situ natural gas steam reforming using Plug flow reactor.



Fig. 4. Graphite core with graphite concentrated at one end (bottom).

2.1.2 Kinetic model description

The kinetic model of hydrogen production through SMR on a Ni-based catalyst supported on alumina is based on Langmuir Hinshelwood reaction mechanism. The reaction scheme consists of two key components: The reversible endothermic SMR reactions and the reversible exothermic WGS reaction represented as follows (Fu et al., 2023):

$$CH_4 + H_2O \rightleftharpoons CO + 3H_2 \quad \Delta H_{298}^\circ = +206 \text{ kJ/mol} \qquad (1)$$

$$CO + H_2O \rightleftharpoons CO_2 + H_2 \quad \Delta H_{298}^{\circ} = -41.1 \text{ kJ/mol} \quad (2)$$

$$CH_4 + 2H_2O \rightleftharpoons CO_2 + 4H_2 \quad \Delta H_{298}^{\circ} = +165 \text{ kJ/mol} \quad (3)$$

Different forms of SMR reaction kinetic equations exist in literature (Szablowski et al., 2025). In this study, two kinetic reaction data given by Xu and Froment (1989) and Hou and Hughes (2001) are used. Details of the reaction rate equations and their expressions in Aspen Plus are given in Supplementary B. The kinetic coefficients and equilibrium constants are presented in Table B2.

The thermodynamic properties were calculated using the RKSMHV2 method, which combines the Redlich-Kwong-Soave equation of state with modified Huron-Vidal mixing rules, suitable for mixtures of polar, non-polar, and light gases (Amrana et al., 2017). The simulation flowsheet is illustrated in Fig. 3. The feed to the SMR reactor consisted of methane and steam with hydrogen to avoid division by zero in the rate expressions. These were mixed in a mixer unit and subsequently heated to the reaction temperature before entering the reactor. The SMR reactor was modeled using the RPLUG block, configured to operate under isothermal conditions. The reactor simulates plug flow behavior by assuming complete radial mixing and is capable of handling three-phase systems (Amrana et al., 2017). The reactor geometry was specified to have a diameter of 2 cm and a length of 10.35 cm, selected

arbitrarily to yield a total volume of 32.5 cm³ and scaled for the porous medium. The catalyst density and bed voidage are specified as 1,870 kg/m³ and 0.4 for Xu and Froment (1989) and 2,797 kg/m³ and 0.44 for Hou and Hughes (2001) kinetics.

2.2 Gas separation studies in graphite samples

2.2.1 Graphite samples

Graphite core samples were prepared using a mixture of cement, silica and graphite (Fig. 4). Two types of samples were made. In one sample, the graphite is concentrated at the outlet end of the core (sample A). This was to simulate the scenario of graphite packing in the production well to selectively produce H₂ and keep CO₂ underground. The second sample has the graphite dispersed evenly in the cement labeled as sample B. This is to assess how distributed graphite influences gas transport and reaction throughout the core, serving as a baseline to isolate the effect of outlet-end packing in sample A.

2.2.2 Gas permeation studies

For permeation studies, a gas permeability system is used as shown in Fig. 5. The study is conducted at ambient temperature with an overburden pressure of 500 psi. Measurements were conducted in two distinct modes: First, single gas permeation was performed by injecting individual gases at varying flow rates, with the corresponding stabilized pressure drops recorded to evaluate intrinsic membrane permeability. Uncertainties of $\pm 6\%$ were assigned for permeability values between 50-1,000 mD and $\pm 10\%$ for values between 1-50 mD based on the setups precision. Second, mixed gas separation was carried out to assess membrane performance under competitive transport conditions. To prepare the required gas mixture, different gases are introduced into a mixing cell one after the other, each at a specified partial pressure. A sample of the mixture is taken, and the composition is confirmed using gas chromatography (GC). The gas mixture is injected into the core and the permeate is collected and analyzed using GC to determine the composition. The data from the two modes of measurements are used to calculate the ideal and real separation factors respectively. The ideal separation factor (α) of the graphite membrane for gas A over a gas B is determined as the ratio of the pure gas permeabilities

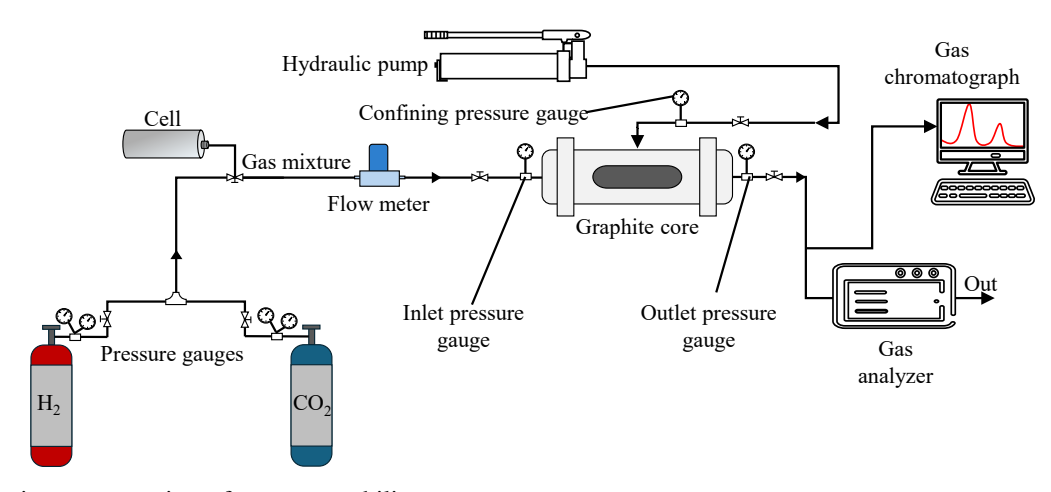


Fig. 5. Schematic representation of gas permeability system.

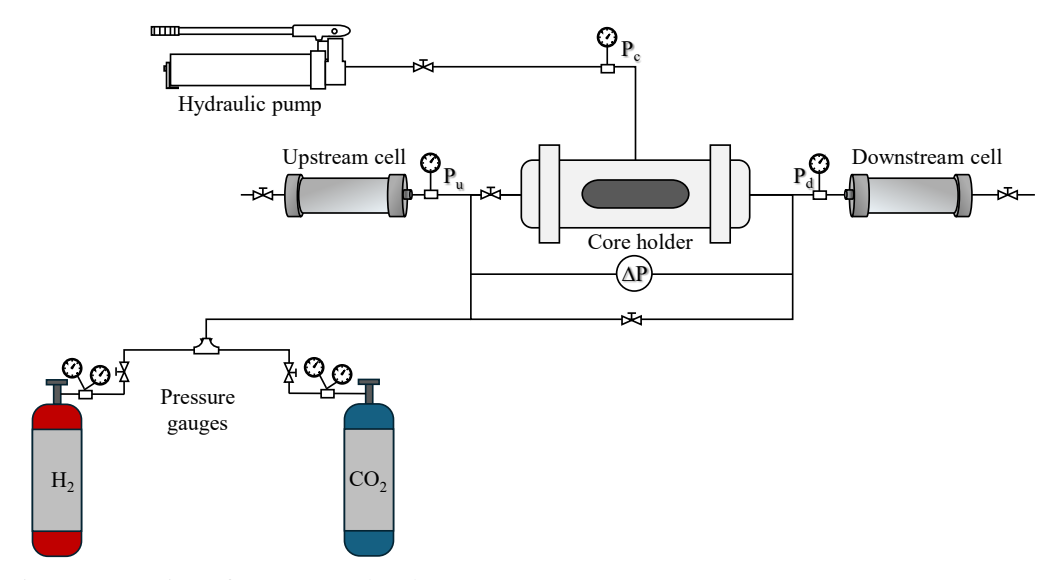


Fig. 6. Schematic representation of pressure pulse decay setup.

(P) as:

$$\alpha_{A,B} = \frac{P_A}{P_B} \tag{4}$$

For the binary gas mixture, the real separation factor is determined in terms of the mole fraction of the gases in the inlet stream (y) and the outlet stream (x) as (Schulz et al., 2014; Malara et al., 2023):

$$\alpha_{A,B} = \frac{y_A/y_B}{x_A/x_B} \tag{5}$$

2.2.3 Gas diffusivity studies

To investigate the molecular-level transport behavior of gases through graphite and gain insights into the underlying gas separation mechanisms, self-diffusivity studies were conducted. Understanding self-diffusivity is essential because it directly reflects the mobility of gas molecules within the graphite structure, which governs separation efficiency, especially in systems where diffusion selectivity dominates over solubility effects. In our previous publication, the diffusivity

of gases through graphite is investigated through molecular dynamic simulation (Raza et al., 2025). A relevant excerpt is included in Supplementary C for the completeness of the gas self-diffusion investigation in the current study. In this study, For this purpose, the Large-scale Atomic/Molecular Massively Parallel Simulator (LAMMPS) was employed due to its robustness in performing molecular dynamics (MD) simulations with high computational efficiency and its ability to handle complex interactions in large atomic systems. While the full details of the MD simulation are presented in a previous publication (Raza et al., 2025), a relevant excerpt is included in this study for the completeness of the gas selfdiffusion investigation in the current study, the diffusivity of the gases is then investigated experimentally by pressure-pulse decay test through graphite core as depicted in Fig. 6. The system comprises an upstream cell with volume V_u and a downstream cell with volume V_d , linked by a core holder that applies hydrostatic confining stress p_c to the graphite core with pore volume V_p . Pressures are monitored with two transducers, each measuring the absolute pressure in the upstream (p_u)

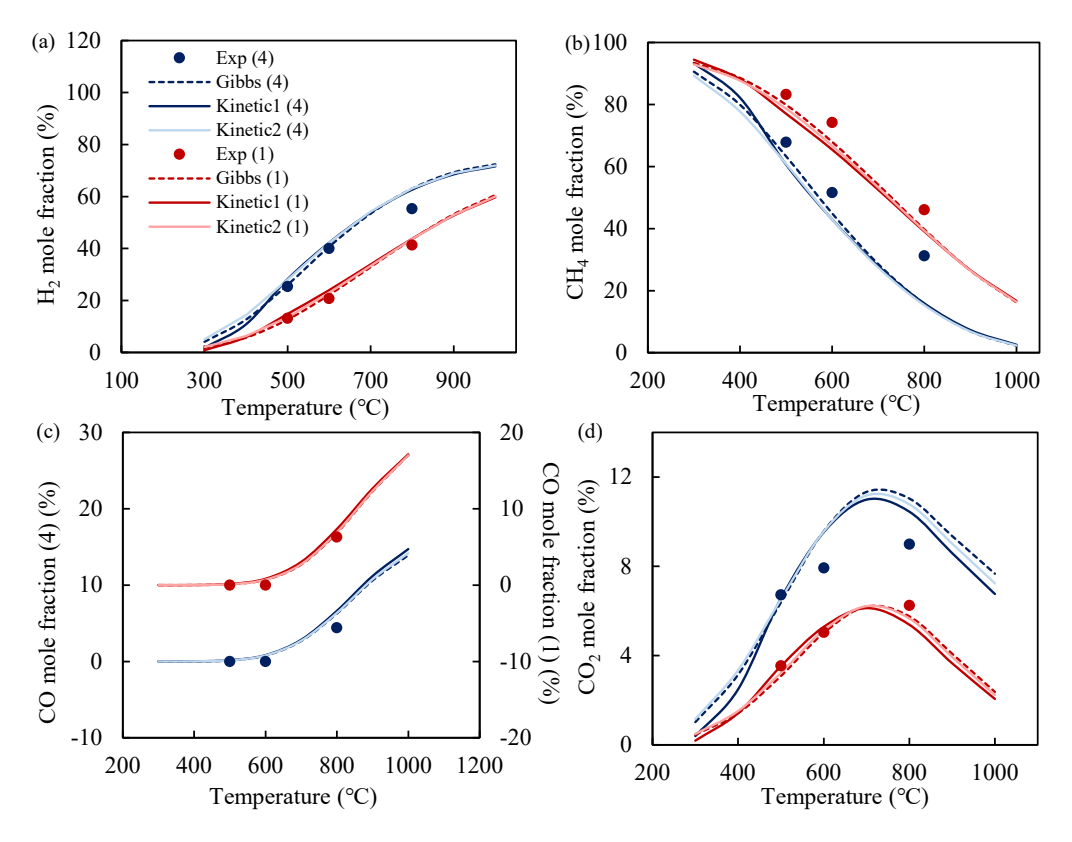


Fig. 7. Comparisons of outflow gas mole fractions (dry basis) (a) H_2 , (b) CH_4 , (c) CO and (d) CO_2 between simulation results (Gibbs and Kinetic) and experimental data (Exp) in literature from Mukhina et al. (2024). The numbers in parenthesis reflect the S/C ratio.

and downstream (p_d) cells. The procedure followed is the typical pressure pulse decay test as presented by Dicker and Smits (Dicker and Smits, 1988). The experiments were run at ambient temperature and 60 °C while the overburden is set at 2,500 psi. The procedure starts with a uniform pressure in the entire system. The pressure in the upstream cell is slightly increased to generate a pressure pulse. As the gas flows through the core, p_u declines until the pulse traverse through the entire core length. Then, p_d starts to increase until the pressure difference (Δp) declines and gradually approaches zero

3. Results and discussion

3.1 Process simulation

This section presents the results of process simulations conducted to investigate IHP from natural gas reservoirs via SR. The simulation model was developed in ASPEN Plus and validated using experimental data from Mukhina et al. (2024), which explored H₂ production under same subsurface conditions. While the referenced experimental study provided valuable insights into reaction behavior at varying S/C ratios and temperatures, the present modeling effort extends that investigation by offering a broader parametric analysis and deeper insight into the thermodynamic behavior of the system under reservoir conditions.

3.1.1 Model validation

To evaluate the predictive accuracy of the process simulation models developed for IHP, the simulation results were validated against experimental data. The validation focuses on the dry mole fractions of the major gaseous components in the outflow stream; H₂, CH₄, CO, and CO₂. The instances for comparison are the three temperatures and two S/C ratios as mentioned earlier. The comparisons between the model predicted mole fractions and the experimental data are presented in Fig. 7. The models successfully reproduce key trends observed in the experimental data. Notably, the models' predictions of H₂ mole fraction for S/C ratio of 4 show strong agreement with the corresponding experimental data except for 800 °C temperature (mean relative error of 5.93%). A stronger agreement is observed for S/C ratio of 1 with a mean relative error of 5.28%. Similarly, the models' predictions of CO mole fraction also show very strong agreement with the corresponding experimental data.

For methane, the model captures the expected consumption trend, with CH₄ mole fraction decreasing as temperature increases. However, the simulations exhibited slightly higher methane consumption compared to experimental results. CO₂ trends are also consistent with established reaction pathways. CO₂ mole fraction rises with temperature, through a maximum around 600-700 °C, likely due to the onset of the reverse water-gas shift (RWGS) reaction at higher temperatures (Maqbool et al., 2021). The models again show better agreement at

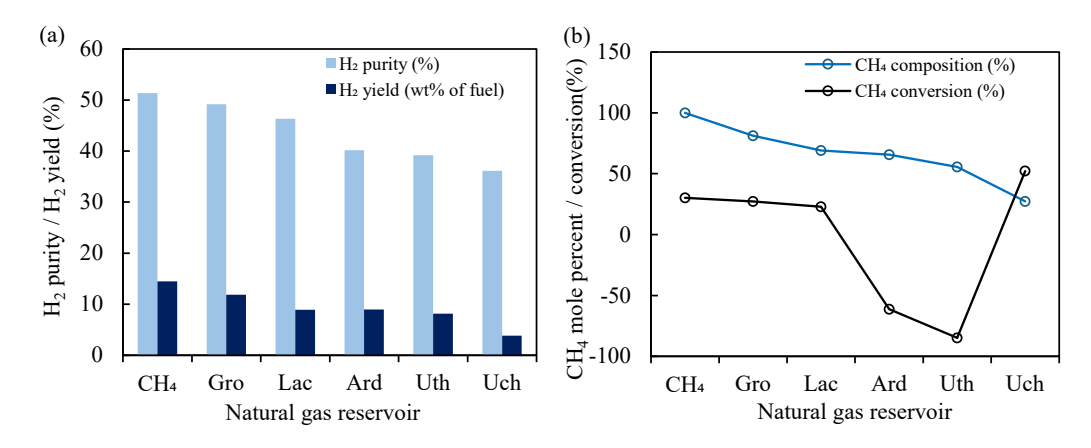


Fig. 8. Effect of natural gas composition on H_2 production: (a) H_2 production for different natural gas composition and (b) CH_4 percentage and conversion in different natural gas composition.

S/C ratio of 1 compared to S/C ratio of 4. The discrepancies between simulated and experimental CH₄ and CO₂ mole fractions likely stem from idealized model assumptions and unmodeled kinetic effects (Ma et al., 2016; Abbas et al., 2017). Catalyst deactivation due to coke formation or sintering, not captured in simulations, reduces methane conversion in practice. Heat and mass transfer limitations create temperature and concentration gradients that lower reaction rates compared to ideal isothermal models. Simplified kinetics that neglect reverse or competing reactions (e.g., RWGS, methanation) further bias results toward higher CO₂ and lower CH₄. Additionally, real experiments experience fluctuations in S/C ratio, temperature, and flow conditions, unlike fixed simulation inputs, leading to greater CH₄ retention and reduced CO₂ generation.

Nevertheless, the simulated results are in close alignment with the experimental data which affirms the models' reliability and scientific validity. Both models showed strong agreement with experimental data despite differing complexities. The RGibbs reactor, based on minimizing Gibbs free energy, is simple, broadly applicable, and ideal for high-temperature, steady-state systems. However, it assumes instantaneous equilibrium, making it less accurate under short residence times or lower temperatures. It also neglects kinetic effects and spatial or temporal variations, which can lead to overestimated gas yields (Żogała, 2014a). In contrast, the RPlug reactor accounts for reaction rates, species concentrations, and time, enabling the modeling of transient behavior and reaction mechanisms. While it offers more realistic predictions in non-equilibrium conditions, it is computationally demanding and highly sensitive to kinetic parameters, which are often difficult to determine and may vary by feed composition. It also requires detailed reaction pathway information, limiting flexibility with unknown or complex feeds (Zogała, 2014b).

3.1.2 Gibbs model analysis

Considering the attributes of the models discussed above, the RGibbs reactor was used to evaluate the impact of natural gas composition on the IHP process. This factor is particularly important because conventional SMR typically utilizes either pure methane, obtained through cryogenic separation or natu-

ral gas with a high methane content to maximize the H_2/CO ratio. In contrast, such preprocessing steps are not feasible in IHP, making the native composition of the underground natural gas a critical parameter in determining the overall efficiency and H_2 yield of the process. The H_2 yield and purity and the conversion of CH_4 are given by the following equations (Abbas et al., 2017):

$$H_{2} \text{ yield (wt.\% of Feed)} = \frac{n_{\text{H}_{2},\text{out}} \times M_{\text{H}_{2}}}{\sum\limits_{i=1}^{n} (n_{i,\text{in}} \times M_{i})} \times 100\%$$
 (6)
$$H_{2} \text{ purity (\%)} = \frac{n_{\text{H}_{2},\text{out}}}{n_{\text{H}_{2},\text{out}} + n_{\text{VG},\text{out}} + n_{\text{CO}_{2},\text{out}}} \times 100\%$$
 (7)
$$CH_{4} \text{ conversion (\%)} = \frac{n_{\text{CH}_{4},\text{in}} - n_{\text{CH}_{4},\text{out}}}{n_{\text{CH}_{4},\text{in}}} \times 100\%$$
 (8)

where $n_{i,\text{in}}$ and $n_{i,\text{out}}$ are the moles of the components in the inflow and the outflow stream. M_{H_2} and M_i are the molecular weights of H_2 and gas components in the feed.

(1) Effect of natural gas composition

The H₂ production yields and purities for different natural gas sources are presented in Fig. 8. As mentioned earlier, methane is the most important component regarding H₂ production from SR. Therefore, the mole fraction of methane in the feed and its conversion during the process are also presented. The mole fraction of methane in the natural gas shows a linear relationship with H₂ yield, and H₂ purity. As expected, pure methane yields the highest H₂ output (51.36%) purity and 14.45% yield) and shows a high methane conversion, demonstrating optimal reforming performance under ideal conditions. Groningen and Lacq, with relatively high methane contents (81.3% and 69%), also show good H₂ yields and H₂ purity, with good methane conversion indicating efficient utilization of available methane. However, the Uch composition exhibited the highest methane conversion, which is attributed to its very low methane mole fraction (27.3%). Consequently, this resulted in the lowest H2 yield and purity among all the natural gas feed.

Furthermore, an interesting anomaly is observed for Ardjuna and Uthmaniyah. Despite following the relationship trend between methane mole fraction with H₂ yield and H₂ purity, a negative methane conversion is observed. This means

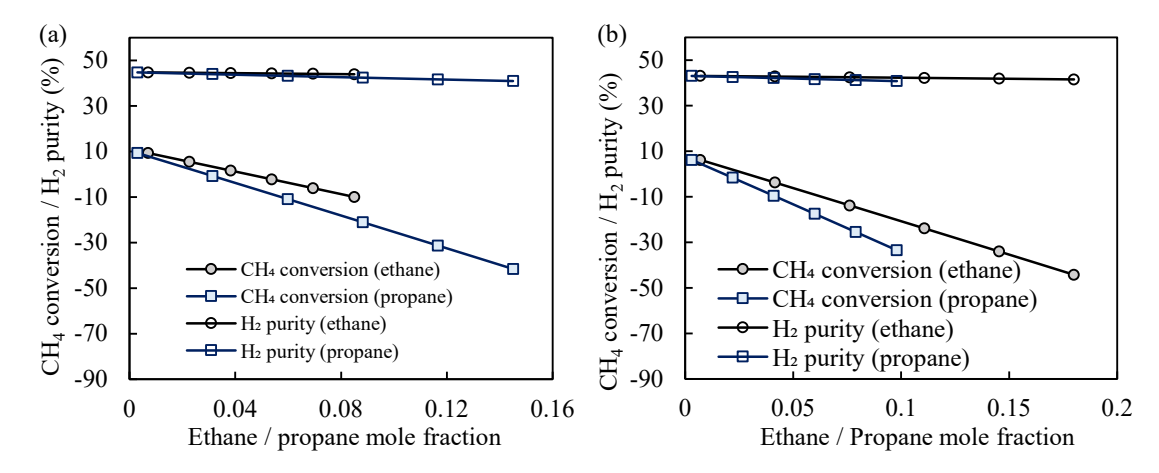


Fig. 9. Impact of other hydrocarbon components' (ethane and propane) mole fraction on methane conversion: (a) Adjuna gas and (b) uthmaniyah gas.

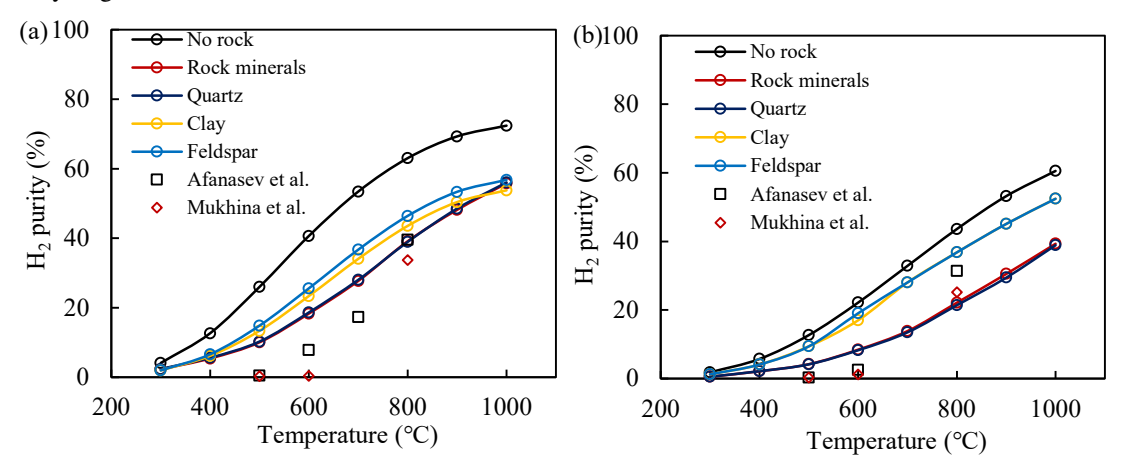


Fig. 10. Impact of rock minerals on IHP at various temperatures for (a) S/C ratio of 4 and (b) S/C ratio of 1. The square and diamond points are experimental data obtained at same thermobaric conditions and rock mineral compositions by Afanasev et al. (2024) and Mukhina et al. (2024) respectively.

more methane was produced than consumed which can be attributed to possible occurrence of methanation reaction at the reaction conditions. A careful look at the compositions of the natural gas sources (Table B1) reveals that these two feeds have higher ethane and propane mole fractions. Based on the stoichiometric reaction, these hydrocarbon components produce higher H₂ compared to methane. However, based on the observed results, their presences in higher percentage facilitate methanation reaction. Similar observation is reported by Adiya et al. (2017) on SR of shale gas containing ethane (16% maximum) and propane (4% maximum) in significant amounts. To validate this inference, the mole fractions of ethane and propane in the natural gas feed were individually varied while keeping the other at a minimal level. The mole fractions of the remaining hydrocarbon components were held constant, and N2 was adjusted accordingly to maintain the overall composition. This approach is justified since N2 does not participate in the H₂ production reactions.

As shown in Fig. 9, increasing the mole fraction of either ethane or propane results in a decline in methane conversion, eventually becoming negative. This shift leads to a reduction in H₂ purity and yield. However, since higher concentrations

of ethane or propane enhance overall H₂ production, their positive contribution offsets the adverse methanation effect. As a result, the net reduction in H₂ output remains minimal. Additionally, propane exhibited a more pronounced effect than ethane, likely due to its higher molecular weight. Methanation reactions are thermodynamically favored under conditions of low temperature and high pressure, which are characteristic of typical reservoir environments (Acierno et al., 2025). Given the conditions examined in this study, the occurrence of methanation reactions is primarily attributed to the high reservoir pressure of 8 MPa. The influence of temperature and pressure on methanation is illustrated in Fig. B1. The results indicate that, at this elevated pressure, the reaction temperature must exceed 900 °C to effectively suppress methanation.

(2) Effect of rock minerals

Introducing rock minerals in the simulation showed an inhibitory effect on the hydrogen production yield as presented in Fig. 10. Irrespective of temperature and S/C ratio, the H₂ yield in the presence of rock minerals is lower compared to the absence of rock minerals. To observe the impact of individual rock minerals, the highest components were also investigated. The quartz-dominated rock sample showed similar impact as

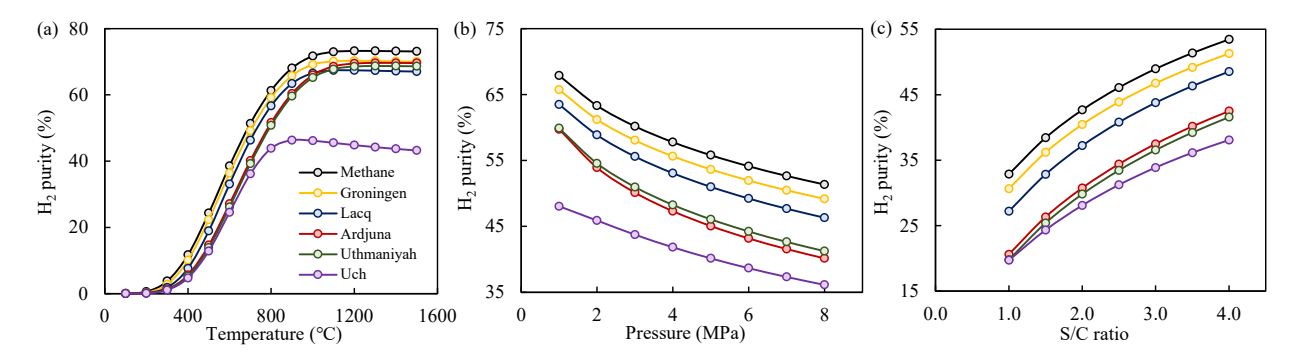


Fig. 11. H₂ purity variation with (a) temperature, (b) pressure and (c) S/C ratio for various natural gas composition.

pure quartz while pure clay and feldspar showed a milder impact. Therefore, the inhibitory impact of the rock sample is predominantly due to the quartz minerals. This observation agrees with reports in literature as shown by the overlaid experimental points in Fig. 10. The overlaid experiments (conducted at same conditions using same rock composition) fall on the mineral curves and below the no-rock envelope. Afanasev et al. (2024) measured ~ 39.6 vol% H₂ at 800 °C, S/C = 4 and ~ 31.2 vol% at S/C = 1 in crushed core, while the simulation reported ~ 39.1 vol% H₂ at 800 °C, S/C = 4 and \sim 22.1 vol% at S/C = 1. Mukhina et al. (2024) likewise found systematically lower H₂ in real core against α-Al₂O₃ under identical conditions. Example at 800 °C, S/C = 4: 33.75 against 55.36 vol% H_2 , with similar gaps at 500-600 °C (\sim 0.33-0.41 against 25.44-39.99 vol%). In fact, the inhibitory impact observed in the experimental studies is higher compared to the simulation owing to other non-ideal factors not accounted for in the simulation.

Mechanistically, the suppression arises from (i) much lower available catalytic surface in real cores compared with α -Al₂O₃ and (ii) rock-derived inhibitors (notably H₂S from sulfur-bearing organics/pyrite) plus coke deposition that weaken/poison Ni and depress conversion (Mukhina et al., 2024). Overall, the simulation corroborates Mukhina et al. (2024) conclusion that native gas-reservoir mineralogy is net-inhibitive for SMR/WGS unless at high S/C ratio and temperature. By contrast, experimental works on other IHP be it heavy oil ISCG (Yang et al., 2022; Jin et al., 2025), or methane cracking (Yan et al., 2024) reported catalytic impact of rock minerals. For example, Jin et al. (2025) in their heavyoil ISCG experiments, reported that plagioclase feldspar and clays often show catalytic behavior (via Fe/Al-bearing phases that promote WGS/coke gasification). Furthermore, Yan et al. (2024) also reported a clear catalytic effect in sandstone, which both lowers the reaction temperature and enhances H₂ production from CH₄ cracking. A detailed reaction pathway analysis is required to clarify the contrasting impact of rock minerals on different IHP processes.

(3) Effect of temperature, S/C ratio and pressure

Temperature has a positive impact on H_2 yield and purity at equilibrium in SR processes. Fig. 11(a) shows the variation of H_2 purity with temperature at constant pressure (8 MPa) and S/C ratio (3.5). All feedstock showed an increase in H_2 purity until a plateau is reached corresponding to complete

conversion of methane followed by WGS (Abbas et al., 2017). This observation is attributed to a transition between dominant reactions specifically, a shift from the strongly exothermic methanation reaction, which is favored at lower temperatures, to the endothermic SMR reaction, which becomes more favorable at elevated temperatures (Adiya et al., 2017). It is worth noting that the other hydrocarbon components show nearly complete conversion irrespective of temperature.

Uch natural gas exhibited a similar temperature-dependent trend; however, beyond a certain temperature threshold: Determined by the prevailing pressure and S/C ratio: The H₂ purity plateaus and begins to decline slightly. This behavior is attributed to the increasing dominance of the RWGS reaction at higher temperatures (Maqbool et al., 2021). Another noteworthy observation is that at elevated temperatures (> 1,000 °C), Ardjuna and Uthmaniyah natural gases exhibited higher H₂ purity than Lacq and approached the levels observed for Groningen, despite having lower methane content. This outcome is attributed to the higher concentrations of ethane and propane in Ardjuna and Uthmaniyah, which contribute additional H₂ through their reforming. Additionally, the methanation reaction is thermodynamically unfavorable at high temperatures, further enhancing H₂ purity under these conditions.

Pressure is another important operating parameter in the SR process. Although direct control over reservoir pressure is limited in IHP, understanding its impact is essential. It enables informed adjustments to other variables, such as temperature and the S/C ratio, to optimize H2 yield and purity under given conditions. Fig. 11(b) shows the variation of H₂ purity with pressure at constant temperature (700 °C) and constant S/C ratio (3.5). In all the natural gas composition, H₂ purity is favored at low pressure. This is because the SR reaction results in an increase in the total number of molecules: From 3 moles of reactants to 4 moles of products. According to Le Chatelier's principle, this shift in molar quantity means that lower pressures favor the forward reaction, as reduced pressure mitigates the increase in total molar concentration and drives the equilibrium toward greater H₂ production. The WGS however is equimolar and therefore insensitive to pressure variation at equilibrium (Abbas et al., 2017). H₂ purity shows a relatively consistent trend across the various natural gas feedstocks at each pressure level. However, as pressure increases, a more pronounced decline in H₂ purity is observed for Ardjuna and Uthmaniyah gases. This is primarily due to

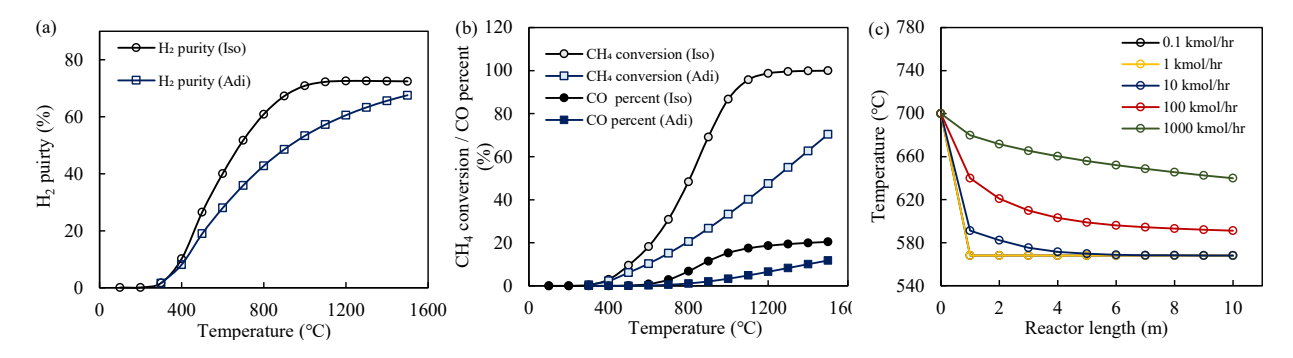


Fig. 12. Impact of temperature on IHP process considering isothermal and adiabatic process: (a) Impact on H₂ purity, (b) impact on CH₄ conversion and CO percentage in syngas, and (c) temperature profile along reactor length at various stream flow rate in an adiabatic process.

the enhanced favorability of the methanation reaction under high-pressure conditions, which consumes H_2 and lowers its overall purity.

The S/C ratio is a critical parameter influencing the overall efficiency of the SR process. Fig. 11(c) illustrates the variation of H₂ purity with S/C ratio at a constant temperature of 700 °C and pressure of 8 MPa. An increase in the S/C ratio enhances SR performance, as evidenced by the rise in H₂ purity. However, higher S/C ratios require greater energy input to generate the necessary steam (Abbas et al., 2017), and excessively high ratios can promote coke deposition on the catalyst surface, leading to catalyst deactivation (Magbool et al., 2021). To balance efficiency and operational stability, maintaining the S/C ratio within the range of 1 to 4 is recommended, which is consistent with findings from previous studies (Adiya et al., 2017). It was also observed that the influence of the S/C ratio varies with the composition of the natural gas feed. At an S/C ratio of 1, Ardjuna, Uthmaniyah, and Uch gases exhibited nearly identical H₂ purity despite differences in their hydrocarbon compositions. However, as the S/C ratio increased, disparities in H₂ purity became more pronounced. The S/C ratio represents the ratio of total moles of water to the total moles of carbon species in the feed. Therefore, feedstocks with higher concentrations of heavier hydrocarbons such as ethane and propane, as seen in Ardjuna and Uthmaniyah, require proportionally more steam to drive reforming reactions effectively.

3.1.3 Kinetic model analysis

The kinetic reactor model was also employed to examine the effects of key operating parameters. In this case, the reactor was modeled as adiabatic to more accurately reflect the conditions of IHP and compared to isothermal model. Unlike the experimental setup by Mukhina et al. (2024) where the system was maintained isothermally using an external furnace, actual subsurface conditions are non-isothermal. In IHP, temperature is initially elevated through ISC but cannot be held constant as the combustion front advances through the reservoir. Additionally, the kinetic model allows the investigation of parameters that could not be captured using the Gibbs reactor, such as catalyst loading and residence time; the latter being influenced by the feed flow rate when other

variables are held constant. The two kinetic models both had good agreement with the experimental data from literature. Therefore, only one model is deployed for this analysis, specifically the model based on Xu and Froment kinetic data.

As expected, temperature has a positive influence on the IHP process, as shown in Figs. 12(a) and 12(b). H₂ purity increases with temperature, mainly attributed to the conversion of methane. The amount of CO in the effluent follows the same trend as the methane conversion, indicating limited occurrence of WGS reaction at high temperature. Similar trends are observed in both the isothermal model and the adiabatic model. However, the H₂ purity is higher in the isothermal model compared to the adiabatic model. While the isothermal system achieves nearly complete methane conversion ($\sim 100\%$) at 1,200 °C, the adiabatic model reaches only about 70% conversion even at 1,500 °C. According to Alekhina et al. (2025), ISC of methane can generate temperatures up to 1,000 °C. Under such conditions, as demonstrated in the adiabatic simulation, a considerable H₂ purity of approximately 53% can still be achieved. In the adiabatic model, temperature decreases along the reactor length as the gas stream progresses. Fig. 12(c) illustrates this behavior for a feed stream entering at 700 °C and flowing through a 10-meter-long reactor at varying molar flow rates. The results show that the gas stream temperature is strongly influenced by the flow rate, primarily due to changes in residence time. At higher flow rates, the residence time is shorter, allowing less heat dissipation and thus maintaining higher temperatures throughout the reactor.

The effect of residence time on the IHP process is illustrated in Fig. 13. Both the isothermal and adiabatic models show that increasing residence time positively influences H₂ purity (Fig. 13(c)). As observed in Fig. 13, increasing residence time increases methane and CO consumption reflected in increasing methane conversion and decreasing CO mole percent respectively (Figs. 13(a) and 13(b)). Initially, H₂ purity increases with residence time and eventually levels off, indicating that extended contact time enhances methane and CO conversion until equilibrium limits are approached. In field-scale IHP applications, long residence times are inherently expected due to the large volume and flow path within the reservoir. This provides a natural advantage for reaction completion, especially when complemented by sufficient thermal input. If

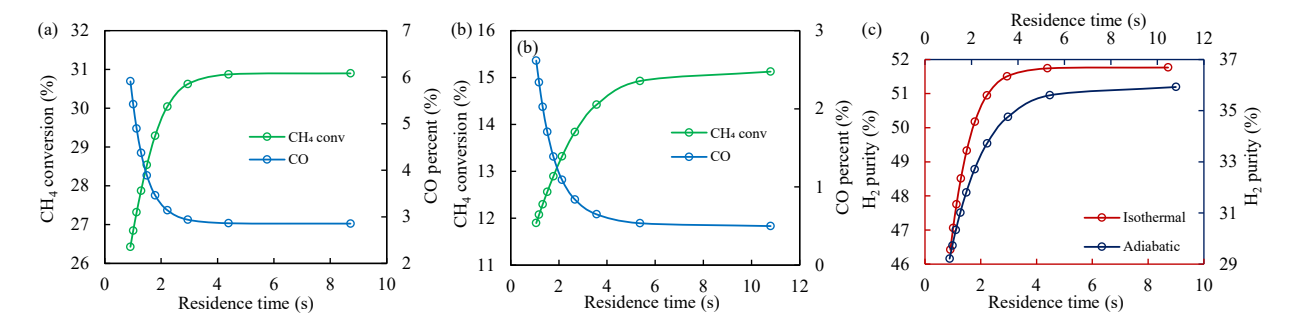


Fig. 13. Impact of residence time on (a) methane and CO consumption under isothermal condition, (b) methane and CO consumption under adiabatic condition and (c) overall H_2 purity.

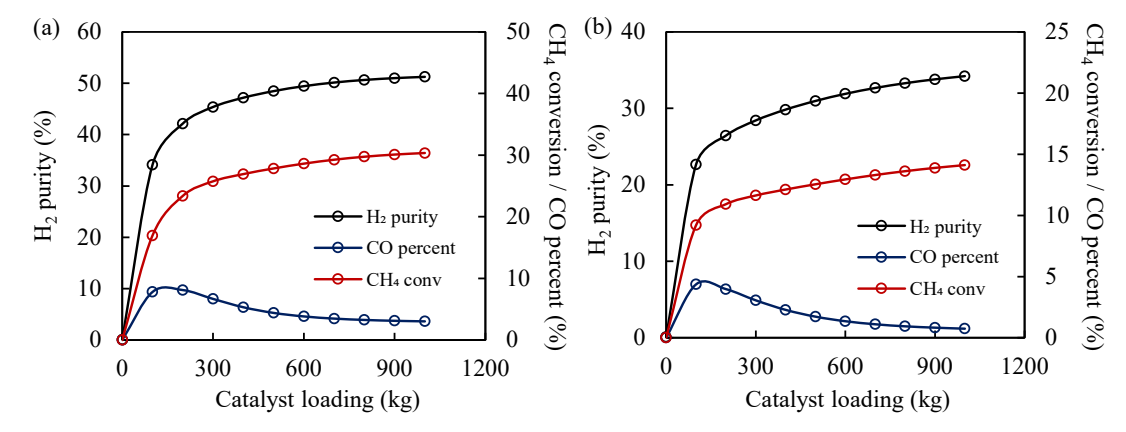


Fig. 14. Impact of catalyst loading on IHP under (a) isothermal condition and (b) adiabatic condition.

ISC generates enough heat to raise the reservoir temperature, subsequent heat dissipation across the formation can sustain elevated temperatures over extended regions. This thermal propagation allows reforming reactions to proceed efficiently even beyond the combustion front. Therefore, understanding the interplay between thermal front movement, heat retention, and fluid residence time is critical for optimizing H₂ yield in large-scale reservoir applications.

Catalyst loading significantly influences H₂ purity with both methane conversion and CO consumption increasing as catalyst weight increases (Fig. 14). This trend is observed under both isothermal and adiabatic conditions. Increasing catalyst loading provides more active sites for the reforming reactions to occur leading to a greater proportion of methane and CO being converted into H₂ (Stutz et al., 2006). Furthermore, a larger catalyst mass can shift the reactions towards the kinetic regime where the reaction rate is more dependent on the intrinsic reactivity of the catalyst and less on external factors like mass transfer (Cherif et al., 2021). However, increasing catalyst weight can introduce diffusion limitations, higher pressure drops, heat transfer challenges, and greater material costs. These factors may reduce reaction efficiency, compromise temperature uniformity, and impact overall system performance and economics (Pashchenko, 2023). In the isothermal model, increasing catalyst weight significantly enhances performance, with H₂ purity exceeding 50% and CH₄ conversion nearing 32% due to ample active sites and stable temperature. In contrast, the adiabatic model shows limited gains; H_2 purity reaches $\sim 33\%$ and CH_4 conversion $\sim 14\%$, as temperature drops along the reactor constrain reaction progress.

3.2 Gas separation

3.2.1 Gas permeation

Before investigating the gas separation ability of graphite, the single-component permeation behavior was first studied. Fig. 15 shows the permeability of the individual gases at different injection rates for the two graphite samples. The permeation of both gases decreases with an increasing injection rate. In both graphite samples, the H₂ permeation is mostly higher than CO₂. However, the difference also decreases with increasing injection rate. As the ratio of the single component permeation, the ideal separation factor as a rough measure of the selectivity of the graphite samples is calculated and presented in Fig. 15. The ideal separation factor decreased with an increasing injection rate owing to increased pressure drop. The high separation factor at a low injection rate is suitable for the graphite application for gas separation. During the selective production of H₂, the gases flow via self-diffusion under the induced pressure differential. The two samples exhibit similar gas separation capability. However, sample B showed slightly better performance owing to the impact of graphite through the entire length of the core. For the binary mixture, the gases are allowed to self-diffuse through the graphite core under differential pressure. The separation property of the graphite core in terms of selectivity $[\alpha(H_2/CO_2)]$, determined by the gas concentrations from the GC analysis, was 2.785.

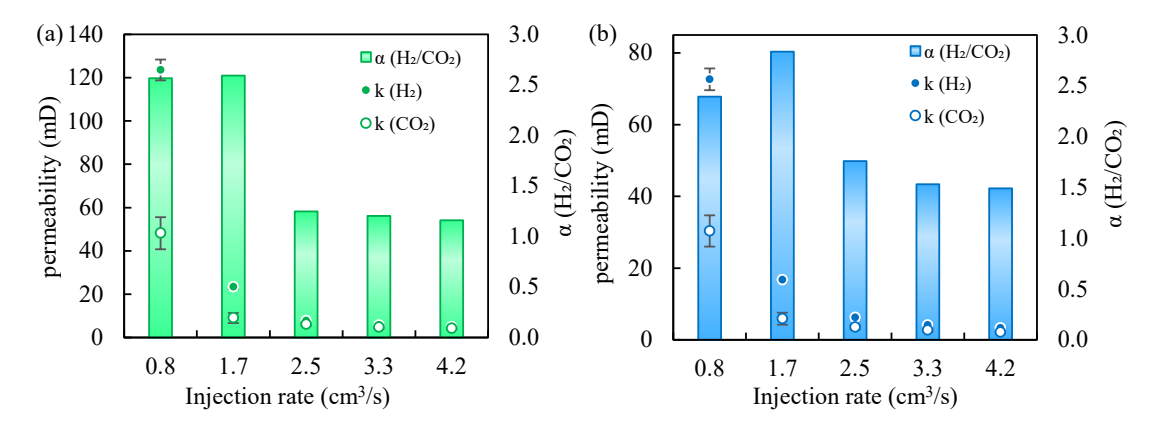


Fig. 15. H₂ and CO₂ single gas permeability and ideal selectivity of (a) sample A and (b) sample B.

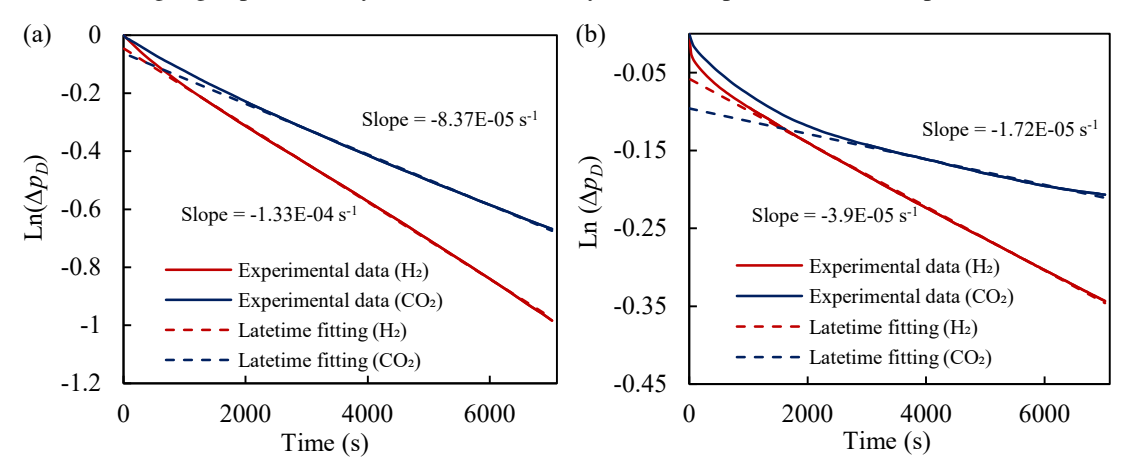


Fig. 16. Semi-log plot of Δp_D against time for effective diffusivity determination at (a) ambient temperature and (b) 60 °C.

 Table 1. Estimated effective diffusivities at different temperature conditions.

Experiment	Slopes (s_1)	Diffusivity (cm ² /s)	Selectivity
CO ₂ @25 °C	-8.38E-05	8.53E-04	1.58
$H_2@25~^{\circ}C$	-1.33E-04	1.35E-03	1.56
CO ₂ @60 °C	-1.72E-05	1.75E-04	2.27
$H_2@60~^{\circ}C$	-3.9E-05	3.97E-04	2.21

3.2.2 Gas diffusivity by pulse decay

Gas diffusivity through the tight graphite core is estimated by fitting the measured $\Delta p(t)$ to the analytical pressure pulse decay solution, using the known cell volumes and core properties as inputs. The detailed analytical solution and derivation can be found in (Cui et al., 2009) and is presented in Supplementary C. The experimental pressure decay data were used to compute dimensionless differential pressures which are then plotted against time on a semi-logarithmic graph. Fig. 16 shows the semi-log plot of Δp_D against time. The effective diffusivities of H_2 and CO_2 and selectivity at different temperatures are presented in Table 1. The diffusion selectivity of the graphite core is low ~ 1.58 at ambient temperature. However, the selectivity is higher at 60 °C (i.e., ~ 2.26). This

observation can be attributed to changes in the phase behavior of gases at different temperature conditions. Depending on the type of gas, the diffusivity could either increase or decrease with temperature. In this study the observed variation of separation factor with temperature is favorable for the intended application.

Furthermore, pressed graphite has been investigated for membrane application in steam reforming of ethanol by Schulz et al. (2014). This study proved that compressing graphite by 392 MPa pressure yield membranes that can give ideal separation factor of ~ 35 -60 and a real separation factor of ~ 5 (Schulz et al., 2014). Therefore, with the availability of high rated pressure compression, a well pressed graphite with improved selectivity can be deployed for gravel packing in a well completion. An important aspect of IHP is the selective production of the generated H₂. All studies and demonstrations have involved membrane technologies which can be very costly and reduce the economic feasibility of this evolving low carbon H₂ production technology. The successful deployment of graphite as gravel packing can improve the economic feasibility of this technology.

4. Conclusions

The feasibility of IHP in natural gas reservoirs was examined using two modeling approaches: A non-stoichiometric equilibrium model (RGibbs reactor) and a kinetic model

(RPlug reactor). Both models reliably reproduced experimental gas compositions (mean relative error < 5.93%), confirming their accuracy. H2 yield and purity increased with CH4 concentration, while heavier hydrocarbons (C₂₊) promoted methanation under high pressure and low temperature, requiring operation above 900 °C for effective CH₄ conversion. Reservoir mineralogy strongly influenced outcomes, with quartz-rich rocks suppressing reforming reactions and clay/feldspar minerals enhancing catalytic cracking. Higher temperatures shifted reactions from exothermic methanation toward endothermic reforming improving hydrogen purity. Lower pressures favored H₂ production, while higher pressures promoted methanation. Increasing the S/C ratio improved yield but raised energy demand and coke risk. Although adiabatic model yielded slightly lower conversions than isothermal model, it better represented reservoir conditions. Longer residence times and higher catalyst loading enhanced CH₄ conversion and H₂ purity. However, optimized catalyst loading prevents diminishing returns, diffusion limitations, and heat transfer challenges.

Secondly, the feasibility of deploying graphite as gravel packing for selective production of H₂ and concurrent storing of associated CO2 was investigated. This approach is believed to be a cost-effective way of improving the carbon neutrality of fossil fuel-based H₂ production methods. Both experimental studies and molecular simulation showed the use of graphite as gravel pack to selectively produce H₂ is an economically viable option to retain CO2 underground and for pressure maintenance to produce H2. Analysis of pressure-decay data indicates H_2/CO_2 diffusion selectivity ~ 1.6 at ambient and ~ 2.3 at 60 °C, consistent with the expectation that selectivity improves with temperature and drops with pressure. While these laboratory values are modest, literature demonstrates that high compaction (~ 392 MPa) can raise performance. This implies that sufficiently pressed graphite can reach applicationrelevant selectivity.

The study therefore corroborates the feasibility of IHP from depleted natural gas reservoirs deploying graphite packing as a cost-effective membrane technology. Although reservoir constraints limit control over feed composition and pressure, the findings of this study show that adjusting temperature and the S/C ratio still enables substantial H₂ yields. For future work, this study could be improved with experimental investigation to generate kinetic data for rock minerals and natural gas components other than methane. While reservoir minerals are known to inhibit H₂ production, the specific mechanisms and the role of individual mineral phases remain unclear. Targeted investigations into mineral-specific effects will be essential for further optimizing IHP performance. Furthermore, the occurrence of methanation reaction proves detrimental to the overall hydrogen yield. Therefore, a deeper thermodynamic and kinetic study of this reaction pathway is recommended to elucidate ways to limit its occurrence at reservoir conditions.

Acknowledgements

The author(s) would like to acknowledge the support provided by the KFUPM Consortium for funding this work

through project No. H2FC2303.

Additional information: Author's email

shahzadmalik@kfupm.edu.sa (M. S. Kamal); uzahid@kfupm.edu.sa (U. Zahid).

Supplementary file

https://doi.org/10.46690/ager.2025.11.06

Conflict of interest

The authors declare no competing interest.

Open Access This article is distributed under the terms and conditions of the Creative Commons Attribution (CC BY-NC-ND) license, which permits unrestricted use, distribution, and reproduction in any medium, provided the original work is properly cited.

References

- Abbas, S. Z., Dupont, V., Mahmud, T. Kinetics study and modelling of steam methane reforming process over a NiO/Al₂O₃ catalyst in an adiabatic packed bed reactor. International Journal of Hydrogen Energy, 2017, 42(5): 2889-2903.
- Acierno, S. G., Finelli, C., Lancia, A., et al. Thermodynamic analysis of CO₂ methanation for power-to-gas applications: Impact of in-situ water removal on performances and heat release. Journal of CO₂ Utilization, 2025, 102: 103226.
- Adiya, Z. I. S. G., Dupont, V., Mahmud, T. Effect of hydrocarbon fractions, N₂ and CO₂ in feed gas on hydrogen production using sorption enhanced steam reforming: Thermodynamic analysis. International Journal of Hydrogen Energy, 2017, 42(34): 21704-21718.
- Afanasev, P. A., Alekhina, T. V, Mukhametdinova, A. Z., et al. Exploring the potential of natural gas reservoirs for underground hydrogen generation. Paper SPE 219113 Presented at the SPE Gas & Oil Technology Showcase and Conference, Dubai, UAE, 7-9 May, 2024.
- Aftab, A., Hassanpouryouzband, A., Xie, Q., et al. Toward a Fundamental Understanding of Geological Hydrogen Storage. Industrial and Engineering Chemistry Research, 2022, 61(9): 3233-3253.
- Alekhina, T., Mukhametdinova, A., Khayrullina, A., et al. Influence of catalyst variation on underground hydrogen generation in gas reservoirs: Impact on hydrogen yield and alteration of catalyst structure and rock properties. International Journal of Hydrogen Energy, 2025, 103: 740-754.
- Algayyim, S. J. M., Saleh, K., Wandel, A. P., et al. Influence of natural gas and hydrogen properties on internal combustion engine performance, combustion, and emissions: A review. Fuel, 2024, 362: 130844.
- AlHumaidan, F. S., Halabi, M. A., Rana, M. S., et al. Blue hydrogen: Current status and future technologies. Energy Conversion and Management, 2023, 283: 116840.
- Amrana, U. I., Ahmadb, A., Othman, M. R. Kinetic based simulation of methane steam reforming and water gas shift for hydrogen production using aspen plus. Chemical

- Engineering, 2017, 56: 1681-1686.
- Aravindan, M., Kumar, P. Hydrogen towards sustainable transition: A review of production, economic, environmental impact and scaling factors. Results in Engineering, 2023, 20: 101456.
- Bashiru, O., Ochem, C., Enyejo, L. A., et al. The crucial role of renewable energy in achieving the sustainable development goals for cleaner energy. Global Journal of Engineering and Technology Advances, 2024, 19(3): 11-36.
- Cherif, A., Nebbali, R., Lee, C. Numerical analysis of steam methane reforming over a novel multi-concentric rings Ni/Al₂O₃ catalyst pattern. International Journal of Energy Research, 2021, 45(13): 18722-18734.
- Cui, X., Bustin, A. M. M., Bustin, R. M. Measurements of gas permeability and diffusivity of tight reservoir rocks: different approaches and their applications. Geofluids, 2009, 9(3): 208-223.
- Dicker, A. I., Smits, R. M. A practical approach for determining permeability from laboratory pressure-pulse decay measurements. Paper SPE 17578 Presented at the SPE International Oil and Gas Conference and Exhibition, Tianjin, China, 1-4 November, 1988.
- Dybkjaer, I. B., Christensen, T. S. Syngas for large scale conversion of natural gas to liquid fuels, in Studies in Surface Science and Catalysis, edited by I. B. Dybkjaer and T. S. Christensen, Elsevier, Netherlands, pp. 435-440, 2001.
- Fu, W. B., Hou, L. Y., Zhong, B. J., et al. An analysis of the ignition of premixed gases by a hot spherical surface with catalytic reforming reaction. Fuel, 2023, 82(5): 539-544.
- Gillick, S. R., Babaei, M. *In-situ* hydrogen production from natural gas wells with subsurface carbon retention. SPE Journal, 2024, 29(4): 2119-2129.
- Gupta, J. G., De, S., Gautam, A., et al. Introduction to sustainable energy, transportation technologies, and policy, in Sustainable Energy and Transportation: Technologies and Policy, edited by A. Gautam, S. De, A. Dhar, J. Gupta and A. Pandey, Springer, Singapore, pp. 3-7, 2018.
- Hajdo, L. E., Hallam, R. J., Vorndran, L. D. L. Hydrogen generation during *in-situ* combustion. Paper SPE-13661 Presented at the SPE Western Regional Meeting, Bakersfield, California, 27-29 March, 1985.
- Hou, K., Hughes, R. The kinetics of methane steam reforming over a Ni/ α -Al₂O catalyst. Chemical Engineering Journal, 2001, 82(1-3): 311-328.
- Howarth, R. W., Jacobson, M. Z. How green is blue hydrogen? Energy Science & Engineering, 2021, 9(10): 1676-1687.
- Ifticene, M. A., Li, Y., Song, P., et al. A new simplified kinetic model for hydrogen generation during in-situ combustion gasification of heavy oil. Paper SPE 220862 Presented at the SPE Annual Technical Conference and Exhibition, New Orleans, Louisiana, USA, 23-25 September, 2024.
- Ifticene, M. A., Yan, K., Yuan, Q. Fueling a carbon-zero future: Igniting hydrogen production from petroleum reservoirs via *in-situ* combustion gasification. Energy Conversion and Management, 2023, 298: 117770.
- Ifticene, M. A., Yuan, Q. Mechanisms of hydrogen generation

- during *in-situ* combustion gasification of heavy oil. Paper SPE 218902 Presented at the SPE Western Regional Meeting, Palo Alto, California, USA, 16-18 April, 2024.
- Ikpeka, P., Ugwu, J., Russell, P., et al. Insitu hydrogen production from hydrocarbon reservoirs-what are the key challenges and prospects? Paper Presented at the 1st Geoscience & Engineering in Energy Transition Conference, Strasbourg, France, 16-18 November, 2020.
- Jin, X., Li, T., Pu, W., et al. Experimental study on the effect of mineral on hydrogen production from heavy oil in-situ combustion gasification. Geoenergy Science and Engineering, 2025, 246: 213612.
- Kumar, R., Kumar, A., Pal, A. An overview of conventional and non-conventional hydrogen production methods. Materials Today: Proceedings, 2021, 46: 5353-5359.
- Liguori, S., Kian, K., Buggy, N., et al. Opportunities and challenges of low-carbon hydrogen via metallic membranes. Progress in Energy and Combustion Science, 2020, 80: 100851.
- Lv, Y. Transitioning to sustainable energy: Opportunities, challenges, and the potential of blockchain technology. Frontiers in Energy Research, 2023, 11: 1258044.
- Ma, R., Castro-Dominguez, B., Mardilovich, I. P., et al. Experimental and simulation studies of the production of renewable hydrogen through ethanol steam reforming in a large-scale catalytic membrane reactor. Chemical Engineering Journal, 2016, 303: 302-313.
- Malara, A., Bonaccorsi, L., Fotia, A., et al. Hybrid fluoro-based polymers/graphite foil for H₂/natural gas separation. Materials, 2023, 16(5): 2105.
- Maqbool, F., Abbas, S. Z., Ramirez-Solis, S., et al. Modelling of one-dimensional heterogeneous catalytic steam methane reforming over various catalysts in an adiabatic packed bed reactor. International Journal of Hydrogen Energy, 2021, 46(7): 5112-5130.
- Massarweh, O., Al-khuzaei, M., Al-Shafi, M., et al. Blue hydrogen production from natural gas reservoirs: A review of application and feasibility. Journal of CO₂ Utilization, 2023, 70: 102438.
- Mukhina, E., Afanasev, P., Mukhametdinova, A., et al. A novel method for hydrogen synthesis in natural gas reservoirs. Fuel, 2024, 370: 131758.
- Nikolaidis, P., Poullikkas, A. A comparative overview of hydrogen production processes. Renewable and Sustainable Energy Reviews, 2017, 67: 597-611.
- Pashchenko, D. Intra-particle diffusion limitation for steam methane reforming over a Ni-based catalyst. Fuel, 2023, 353: 129205.
- Raza, A., Alafnan, S., Mahmoud, M., et al. Diffusive nature of different gases in graphite: Implications for gas separation membrane technology. Journal of Industrial and Engineering Chemistry, 2025, 144: 526-540.
- Riemer, M., Duscha, V. Carbon capture in blue hydrogen production is not where it is supposed to be-Evaluating the gap between practical experience and literature estimates. Applied Energy, 2023, 349: 121622.
- Satpute, M., Suryabhan, S. Environmental degradation and renewable energy. International Journal of Advanced

- Research in Science, Communication and Technology, 2024, 4(1): 160-165.
- Schulz, A., Steinbach, F., Caro, J. Pressed graphite crystals as gas separation membrane for steam reforming of ethanol. Journal of Membrane Science, 2014, 469: 284-291.
- Soltani, S. M., Lahiri, A., Bahzad, H., et al. Sorption-enhanced steam methane reforming for combined CO₂ capture and hydrogen production: A state-of-the-art review. Carbon Capture Science & Technology, 2021, 1: 100003.
- Stutz, M. J., Hotz, N., Poulikakos, D. Optimization of methane reforming in a microreactor-effects of catalyst loading and geometry. Chemical Engineering Science, 2006, 61(12): 4027-4040.
- Szablowski, L., Wojcik, M., Dybinski, O. Review of steam methane reforming as a method of hydrogen production. Energy, 2025, 316: 134540.
- Tackie-Otoo, B. N., Mahmoud, M., Murtaza, M., et al. An integrated experimental and simulation study for the feasibility of underground H₂ production from natural gas reservoirs. ACS Omega, 2025, 10(23): 24510-24519.
- Tarkowski, R., Uliasz-Misiak, B. Towards underground hydrogen storage: A review of barriers. Renewable and

- Sustainable Energy Reviews, 2022, 162: 112451.
- Tong, X., Zhang, G., Wang, Z., et al. Distribution and potential of global oil and gas resources. Petroleum Exploration and Development, 2018, 45(4): 779-789.
- Xu, J., Froment, G. F. Methane steam reforming, methanation and water-gas shift: I. Intrinsic kinetics. AIChE Journal, 1989, 35(1): 88-96.
- Yan, K., Yang, X., Ge, Y., et al. Iron-sandstone synergy: Advancing *in-situ* hydrogen production from natural gas via electromagnetic heating. International Journal of Hydrogen Energy, 2024, 83: 1210-1218.
- Yang, S., Huang, S., Jiang, Q., et al. Experimental study of hydrogen generation from *in-situ* heavy oil gasification. Fuel, 2022, 313: 122640.
- Zogała, A. Critical analysis of underground coal gasification models. Part I: Equilibrium models-literary studies. Journal of Sustainable Mining, 2014a, 13(1): 22-28.
- Żogała, A. Critical analysis of underground coal gasification models. Part II: Kinetic and computational fluid dynamics models. Journal of Sustainable Mining, 2014b, 13(1): 29-37.